



Membrane modification by liquid phase deposition using small amount of TiO₂ for high-temperature operation of polymer electrolyte fuel cells

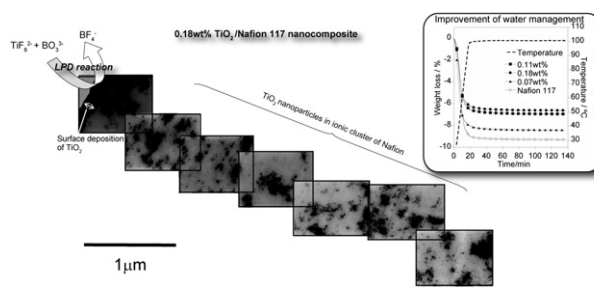
Takashi Hasegawa, Alexis Bienvenu Béléké, Minoru Mizuhata*

Department of Chemical Science and Engineering, Graduate School of Engineering, Kobe University, 1-1 Rokkodai-cho, Nada, Kobe 657-8501, Japan

HIGHLIGHTS

- We prepared TiO₂-dispersed Nafion membrane by the liquid phase deposition method.
- Such membrane can improve the water management by existing hydrophilic filler.
- The amount of loading TiO₂ is much lower than previous reports.
- Water management was much improved after deposition despite the amount was so low.
- This material can contribute to PEFCs operating at high temperature.

GRAPHICAL ABSTRACT



ARTICLE INFO

Article history:

Received 20 November 2012
Received in revised form
17 January 2013
Accepted 19 January 2013
Available online 28 January 2013

Keywords:

Nafion membrane
Inorganic filler
Nanoparticles
Polymer electrolyte fuel cells
Liquid phase deposition

ABSTRACT

A TiO₂-dispersed Nafion (Nafion–TiO₂) membrane is prepared by the liquid phase deposition (LPD) method by carrying out a hydrolysis reaction of titanium–fluoro complex in an aqueous solution. The conductivity of the TiO₂-modified membrane is studied. The obtained composite membrane has dispersed TiO₂ nanoparticles which enhance the membrane's hydrophilic and hygroscopic properties of polymer electrolyte fuel cells (PEFCs) under high temperature conditions. Change in the amount of TiO₂ deposited on the Nafion membrane from 0.07 to 0.18 wt% for LPD reaction periods ranging from 3 to 9 h does not result in any change in the membrane's ion-exchange capacities. High resolution transmission electron microscopy (HRTEM) images indicate the growth and agglomeration of TiO₂ particles at the surface during the LPD reaction. The diffusion of TiO₂ is observed in the membrane from its surface up to a depth of ca. 20 μm by means of XPS measurement. The water retention capacity of the membrane is improved from 63% to 83% at 200 °C by the deposition of 0.18 wt% of TiO₂. Consequently, we find the small amount of TiO₂ improved water management and increase the proton conductivity.

© 2013 Elsevier B.V. All rights reserved.

1. Introduction

Polymer electrolyte fuel cells (PEFCs) are considered to be promising candidates for clean and efficient power generation. However, several factors; such as cost, reliability, and durability pose major challenges in the commercialization of PEFCs [1]. The core

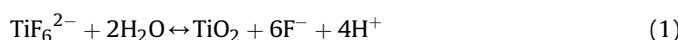
component of PEFCs is the polymeric membrane that functions as a charge carrier for protons, a separator for the reactant gases, and an electronic insulator that prevents electrons from passing through [2]. Perfluorinated sulfonic acid (PFSA) polymers such as Nafion (from DuPont) are the most commonly employed electrolyte membranes for PEFCs operating in ambient temperatures of less than 80 °C; Nafion exhibits good chemical stability, high mechanical strength, and high proton conductivity under well-humidified conditions [3,4]. However, it is known that PEFCs operating at temperatures higher than 100 °C offer significant advantages such

* Corresponding author. Tel./fax: +81 78 803 6186.

E-mail address: mizuhata@kobe-u.ac.jp (M. Mizuhata).

as reduced CO poisoning at the anode, increased energy efficiency, improved heat rejection, improved quality of waste heat, and easy water management control [5,6]. In order to achieve good performance at high temperatures, the PFSA membranes need to be fully wet because proton conduction in the membrane relies on the dissociation of protons from the sulfonic acid groups (SO_3H) in the presence of water. Cell operation at temperatures around 100 °C causes dehydration of the PFSA membranes, thereby resulting in a rapid loss of conductivity and leading to degraded cell performance. Therefore, it is necessary to develop a proton exchange membrane for high-temperature fuel cell applications. Many studies have focused on the development of such membranes. A number of these researches have dealt with the modification of PFSA membranes in order to meet the operational requirements of high-temperature fuel cells. Hybrid Nafion-inorganic oxide electrolytes belong to this category [7]. The preparation of organic–inorganic membranes by incorporating hygroscopic metal oxide particles such as TiO_2 [7–11], ZrO_2 [7,8], SiO_2 [8–13], and other such materials [7,14–16] into membrane resin is considered one of the most effective approaches to ensure a certain relative humidity (RH) in cells operating at temperatures above 100 °C. In such electrolytes, the contribution of ceramic nanoparticles to increased PEFC performance at high temperature is frequently attributed to both the enhanced water retention and improved transport properties of the electrolyte. The most common technique in the modification of a PFSA membrane by incorporation of inorganic oxides is the use of the in-situ sol–gel method; this method results in higher water retention. This technique consists of complex procedures such as the use of an organic solvent, hydration, and heating [8,10–13]. While several researchers have focused on the water retention capabilities of the membrane, very few have considered focusing on the quantity and distribution of inorganic fillers throughout the inner region of the membrane. These inorganic fillers may affect the membrane's intrinsic properties to a certain extent and lead to a reduction in the proton conductivity and mechanical strength of the membrane. The quantity of inorganic fillers used in previous studies has been in the range of 2.5–25 wt% [7–15], and it has been found that, for a fixed level of water content, the proton conductivity in the membrane depends on the quantity of inorganic filler used. Therefore, the filler content should be reduced to a minimum level in order to maintain the ionic conductivity.

In order to improve these abovementioned properties of the PFSA membrane, we fabricated a TiO_2 -dispersed Nafion membrane with high hydrophilic and hygroscopic properties using the liquid phase deposition (LPD) method. It is well-known that the LPD method is the one of the available soft solution processes for the preparation of metal oxides and/or thin films with large surface area and complex morphology [17,18]. TiO_2 thin films can be prepared by a simple and ambient process that involves the following two reactions, therefore hydrolysis of metal-fluorocomplex (1) and reaction of fluorine scavenging (2) [18]:



In this reaction process, the metal oxide species (TiO_2) infiltrate into the nano-sized spaces in the electrolyte. The reaction solution can penetrate the micro or nanopores in various kinds of substrate materials and on the surface of each pore. Deki et al. have developed such a deposition process by means of the liquid phase infiltration method using nano-ordered templates such as 2D arrays or trench structures prepared by deep reactive ion etching (RIE) [19,20], inverse opal structures using 3D colloidal

crystals [21], nano-ordered oxide species using inverse micelles [22], the addition of aqueous polymer solution [23], and on-site synthesis using solid fluorine scavenger [24]. In such cases, the LPD method realized the deposition on the soft matter surface including polymer substrate. Additionally, the LPD method has been applied for fabrication of organic–inorganic composite materials [25].

In this study, the TiO_2 nanoparticles are embedded in the vicinity of the membrane surface. Such a unique incorporation state is thought to be important because the membrane is required to maintain its intrinsic properties such as conductivity and ion exchange capacity, especially at the inner region. Therefore, the oxide amount in the membrane is reduced by the deposition of the metal oxide (by the LPD process) in limited spaces such as the ion-channel structure. Further, we have attempted to improve water management in the process without changing the membrane's intrinsic properties (such as ion exchange capacity and proton conductivity) with LPD process.

2. Experimental

2.1. Samples

As a substrate matrix polymer, Nafion® 117 (DuPont) was pre-treated by immersion and stirring in mixed aqueous solution of 1.0 mol dm^{-3} HNO_3 and 1.6 mol dm^{-3} H_2O_2 at 70 °C for 1 h. Afterward the membrane was washed using distilled water at 70 °C for 1 h. Subsequently, this pretreatment procedure was done twice. The pretreated Nafion membrane was cut into 20 mm × 20 mm for LPD reaction.

For preparation of the parent solutions for the LPD reactions, $(\text{NH}_4)_2\text{TiF}_6$ (Morita Chemical Industries Co. Ltd.) and H_3BO_3 (Nacalai Tesuque Inc.) were dissolved and diluted in deionized distilled water purified by Advantec GSH-200 to give concentrations of 0.5 mol dm^{-3} . Aqueous H_3BO_3 solution was added to aqueous $(\text{NH}_4)_2\text{TiF}_6$ solution for the LPD reaction. The final concentrations of $(\text{NH}_4)_2\text{TiF}_6$ and H_3BO_3 in reaction solution were 0.1 mol dm^{-3} and 0.2 mol dm^{-3} , respectively.

For the preparation of TiO_2 -dispersed Nafion, a piece of Nafion® 117 membrane was immersed in 20 ml of the reaction solution at 30 °C. Reaction periods ranged from 3 to 9 h. Each prepared membrane was thoroughly washed by ion-exchange water and dried in a vacuum oven at 100 °C for 6 h.

2.2. Quantitative analysis of ionic species

We employed inductive coupled plasma atomic emission spectrometry (ICP-AES; Horiba Ultima 2000) for quantitative analysis of ionic species in reaction solution. The membrane was immersed into 1.0 mol dm^{-3} HCl solution. After all cationic species eluted in the HCl solution, the amount of dispersed TiO_2 in the membrane was measured by ICP.

A neutralization titration was carried out in order to determine the ion-exchange capacity of the membrane. Since ammonium ions were remained in Nafion membrane after LPD reaction using $(\text{NH}_4)_2\text{TiF}_6$, the membranes were immersed in 0.1 mol dm^{-3} citric acid aqueous solution for 12 h to ion-exchange into proton for normalization three times. The H^+ form membrane was immersed in 2.0 mol dm^{-3} NaCl (Nacalai Tesuque Inc.) and 0.01 mol dm^{-3} NaOH aqueous solution titrated with phenolphthalein.

2.3. Observation of deposited TiO_2

Distribution and elemental analysis of dispersed TiO_2 in Nafion were observed by cross-sectional SEM imaging and elemental

analysis by field emission scanning electron microscopy (FE-SEM; JEOL JEM-6335F) with energy-dispersive X-ray spectroscopy at an accelerating voltage of 15 kV (SEM-EDX; JEOL EX-23000BU). The dispersion condition of TiO₂ in Nafion was observed by transmission electron microscopy (TEM; JEOL JEM-2000) at an accelerating voltage of 200 kV. The TEM images were enhanced and analyzed digitally using ImageJ software provided by National Institute of Health (NIH).

In order to discuss the effect of ion cluster channel by the LPD reaction, we carried out small angle X-ray scattering (SAXS; AntonPaar Saxscess) measurements by means of on line collimation by the optical alignment of a Kratzky camera. Kratzky camera we use is basically consisted with the vacuum chamber, CuK α X-ray tube with multilayer mirror, beam collimation blocks, and direct beam stopper. Membrane samples were placed in the X-ray pathway under vacuum conditions in order to avoid detection due to X-ray scattering by gas molecule. The scattering intensity was recorded by the imaging plate mounted along the circular with radius of 263.3 mm (corresponding to the distance between sample and detector). After exposure for 20 min, the imaging plate was mounted to the imaging-plate detection system (Cyclone, Storage Phosphor System from Perkin Elmer). The scattering profile was obtained on the length and recalculated them on following scattering vector $q \text{ nm}^{-1}$. Here q is the magnitude of the scattering wave vector which defined as

$$q = 4\pi/\lambda \sin(\theta/2) \quad (3)$$

where θ is the scattering angle and λ is the wavelength of X-ray. The SAXS profile was obtained by integrating the intensity from obtained images. The value of $q = 0$ ($\theta = 0$) was set at the direct beam line. The intensity $I(q)$ is calculated by the following equation.

$$I(q) = I^*(q)/I_0 \quad (4)$$

where $I^*(q)$ and I_0 are measured intensity calculated from SAXS image and intensity at $q = 0$ obtained from attenuated direct beam, respectively.

X-ray photoelectron spectroscopy (XPS; JEOL JPS-9010MC) studies were carried out using MgK α source. The depth profiles were obtained by XPS using an Ar $^{+}$ etching gun at an acceleration voltage of 500 V. The etching rate was measured by SEM and estimated to be ca. 1 $\mu\text{m}/\text{etching}$. The depth profiles were illustrated from the mean value of five measurements. The integral intensity was plotted for the etching time after normalization at the surface (depth = 0).

2.4. Water uptake of TiO₂-modified Nafion

The as-deposited samples were characterized from the point-of-view of the deposition mechanism, while the re-exchanged membrane samples (re-exchanged by immersion in citric acid) were used for the investigation of their ion exchanging capacity and water uptake performance. The fully hydrated water uptake value was obtained by gravimetric analysis after the samples were dried in a vacuum oven at 100 °C for 6 h; this value was calculated using Eq. (5):

$$(\text{Water uptake} = 100(W_f/W_0 - 1)) \quad (5)$$

Here, W_0 and W_f represent the weights of the membrane before and after the complete hydration procedure [16]. Thermal gravimetry (TG) was employed in a temperature range from room temperature to 300 °C with a 5 °C min $^{-1}$ scan rate using the Rigaku

Thermo Plus TG 8120. We defined the membrane's water holding capacity using Eq. (6).

$$\text{Water holding capacity} = 100[(W - W_0)/(W_f - W_0)] \quad (6)$$

where W is the weight of the membrane obtained at each temperature in the TG scanning process.

2.5. Measurement of proton conductivity

The proton conductivity of the membrane was measured using the ac impedance method. Platinum electrodes were used as working electrodes in Zawodzinski's specialized cell [26], and the cell was connected to an ac impedance system (Ivium Compact Stat). The proton conductivities of the membrane were measured over a gradually increasing temperature range from 80 °C to 98 °C. The distance between two platinum electrodes was fixed at 5 mm. The test membrane (10 mm × 10 mm) was placed between the two electrodes. The cell was set up in a humidity chamber (Espec SH221) and 100% RH was maintained at each temperature. A Nyquist plot was drawn in the frequency range of 1.5 MHz–100 Hz. We analyzed the semicircular section of the Nyquist plot, and we used the following equation to obtain the values of conductivity (σ).

$$\sigma = \frac{1}{R} \times \frac{d}{tl} \quad (7)$$

Here, R corresponds to the resistance value of the smaller edge in the semicircles in the Nyquist plot. Further, d denotes the distance between the two electrodes, t denotes the thickness of the membrane, and l denotes the length of the membrane, respectively. In our calculations of proton conductivity, we assumed the thickness value of all the membrane samples to be 180 μm .

3. Results and discussion

3.1. Variations of deposition amount of TiO₂ on Nafion 117 membrane with LPD reaction time

The oxide content in the membrane obtained from the LPD process was much less than that obtained from the sol–gel method, because organic compounds that cause membrane swelling were not used in the LPD process. The amount of TiO₂ deposited and its properties related to the membranes (including Nafion 117) after LPD reactions for various durations are shown in Table 1. The contents of TiO₂ in the membrane increased from 0.074 to 0.18 wt% with increasing LPD reaction period. This range of values is much less than that obtained from the sol–gel method by around 10 wt% [9]. The ion-exchange capacities did not change significantly with increase in TiO₂ deposition amounts. These results cause improvements in the water management properties of Nafion due to an existence of inorganic fillers (incorporated by LPD) with no influence of ion-exchanging properties of the membrane.

Table 1
Properties of membranes after TiO₂ deposited including Nafion 117.

LPD reaction time (h)	TiO ₂ weight ratio (wt%)	Ion exchange capacity (meq g $^{-1}$)	Fully hydrated water uptake (wt%)
Original	—	0.91	27.5
3	0.07	0.92	23.7
6	0.11	0.93	24.6
9	0.18	0.93	31.9

3.2. Distribution of deposited TiO_2 in membrane

The SEM image and EDX line profile of Ti in the Nafion- TiO_2 composite after a reaction period of 9 h is shown in Fig. 1. Although most of the TiO_2 deposition was confined to the surface of Nafion membrane, a certain amount of TiO_2 penetration can be observed in the EDX line profile of the membrane.

The cross-sectional TEM images of the vicinity of the membrane's surface after LPD reactions for 3 h and 9 h are shown in Fig. 2. A large amount of TiO_2 deposition is visible at the surface along with the accumulation of TiO_2 nanoparticle aggregates at the edge of the Nafion membrane. Fig. 2a shows TiO_2 deposition after 3 h; TiO_2 nanoparticles with diameters of 5–30 nm are well-dispersed at both the surface and throughout the depth (the inner region) of the membrane. Further, it is observed that increasing the reaction period to 9 h causes aggregation of the TiO_2 particles. Thin films with mean thickness of 108 nm and 139 nm are deposited for reaction periods of 3 h and 9 h, respectively. The aggregation and formation of TiO_2 particles are clearly visible in both cases. Nano-sized crystallites were observed in both the deposited TiO_2 layer on the surface of the membrane (as shown in Fig. 2c) and in the dispersed nanoparticles observed throughout the depth of the membrane (the corresponding high resolution TEM images are shown in Fig. 3). As shown in Fig. 2c, the highlighted section in the FFT image indicates the existence of the 101 plane of anatase TiO_2 .

The particle aggregation in the inner regions of the membrane is assumed to be caused by the increasing amount of TiO_2 deposition

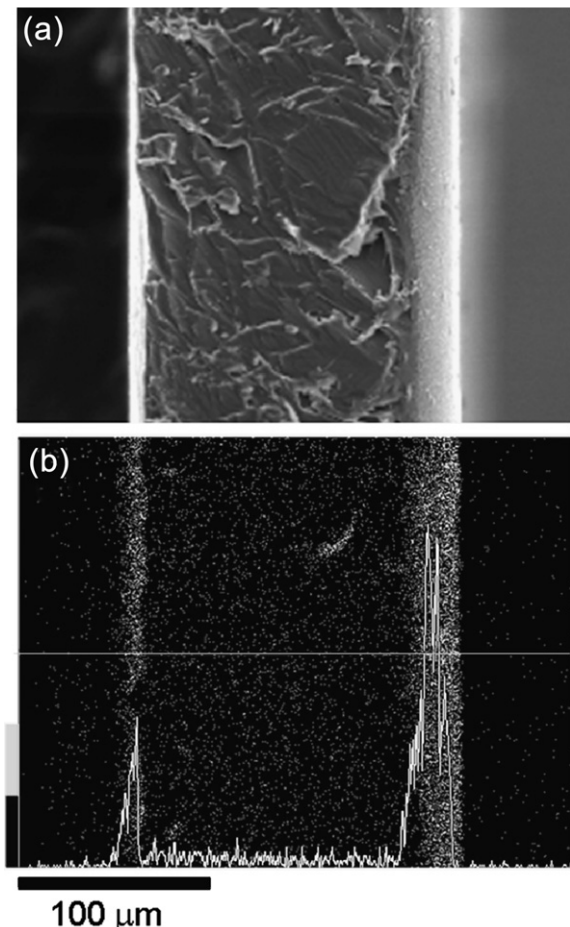


Fig. 1. (a) Cross-sectional SEM image and (b) its EDX profile obtained from $\text{TiK}\alpha$ emission from the TiO_2 -modified Nafion membrane after 9 h reaction.

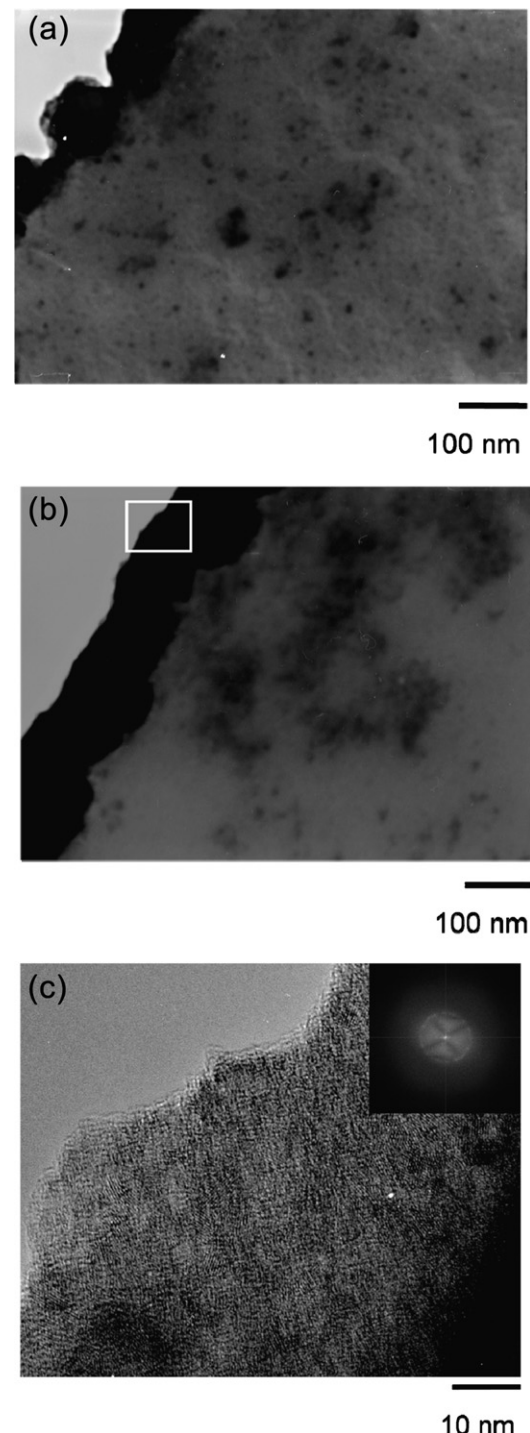


Fig. 2. Cross-sectional TEM images of Nafion containing TiO_2 nanoparticles at two different reaction periods; (a) 3 h and (b) 9 h. (c) High magnification image of the square area in (b), and FFT image of TEM image (c) (inset).

in the bulk solution. Fig. 2c shows the TEM micrograph of the interface between the surface of Nafion and the bulk solution after 9 h of reaction.

In order to examine the distribution of the TiO_2 particles on the membrane, we analyzed TEM images digitally after enhancing and simplifying them. The black areas in Fig. 4 represent the aggregation area of TiO_2 or the existence of their nanoparticles. As observed in Fig. 4, the 7 selected regions (Fig. 4a–g) show particle aggregation at varying distances from the membrane surface; the distances

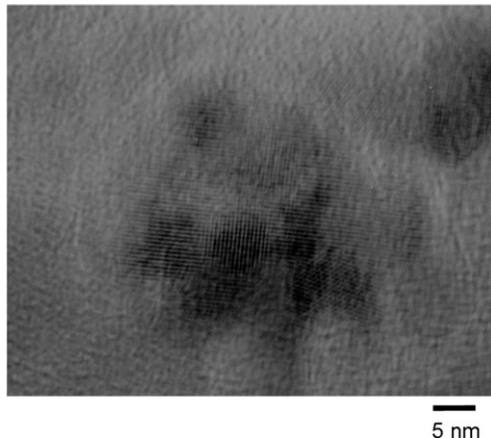


Fig. 3. Cross-sectional TEM image of aggregation within Nafion membranes after 9 h of LPD reaction. The lattice fringes seen in this image are assigned to 101 of anatase TiO₂.

in each case are as follows: (a) $0.45 \pm 0.45 \mu\text{m}$, (b) $1.15 \pm 0.55 \mu\text{m}$, (c) $1.90 \pm 0.50 \mu\text{m}$, (d) $2.50 \pm 0.60 \mu\text{m}$, (e) $3.25 \pm 0.65 \mu\text{m}$, (f) $4.20 \pm 0.60 \mu\text{m}$, and (g) $5.05 \pm 0.55 \mu\text{m}$.

In each TEM image, the area fraction occupied by the deposited oxide particles decreased with the distance from the surface (as shown in Fig. 4h); this area fraction was calculated from the image analysis of each TEM image (using ImageJ) in Fig. 4a–g.

Furthermore, it is observed that the state of dispersion from aggregation to well-dispersed nanoparticles depends on the

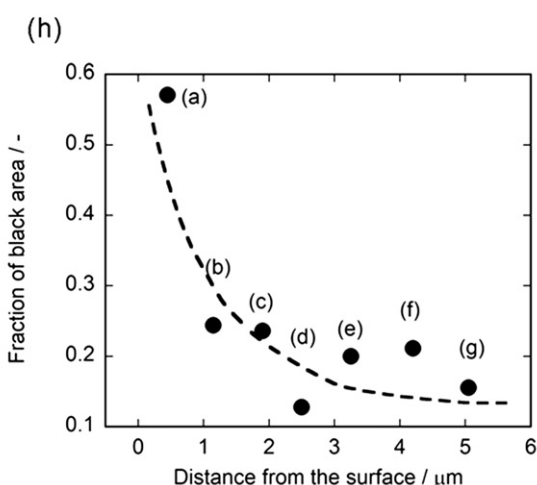
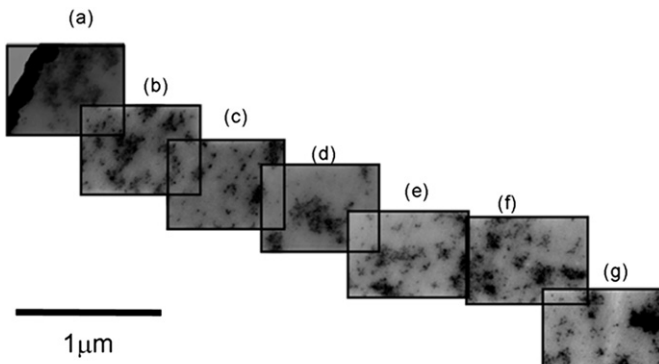


Fig. 4. (a–g) Cross-sectional TEM images of the membrane sample after LPD reaction for 9 h for varying sampling depths indicated in Table 2 and (h) variation in the fraction of aggregation area based on the distance from the membrane surface.

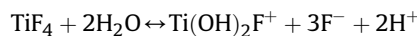
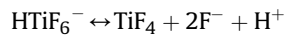
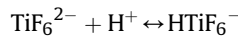
Table 2

Particle size dependence on the distance from the membrane surface. Each value was obtained from the TEM image in Fig. 4.

Position	Distance from surface (μm)	Particle size (nm)	
		Mean size	S.D.
a	0.45	—	—
b	1.15	18.3	7.4
c	1.90	18.3	5.0
d	2.50	13.3	3.4
e	3.25	17.8	6.2
f	4.20	18.5	6.2
g	5.05	17.0	7.3

distance of the dispersion from the surface. It is noteworthy that the sizes of the first order particles remain almost unchanged (as observed from Table 2). These results are corroborated by the SEM-EDX images shown in Fig. 1.

The hydrolysis equilibrium of TiF_6^{2-} are shown in the following reaction [27]



The cation species ($\text{Ti(OH)}_2\text{F}^+$) might exist in the system. In case of adding H_3BO_3 , the hydrolysis reaction should be shifted to the right side in the abovementioned equilibrium by F^- scavenge reaction. The concentration of hydroxo titanium would increase and diffuse into membrane inner region. As Sugimoto et al. reported the presence of Ti(OH)_3^+ by UV-vis technique, titanium hydroxo complex leads to the dehydration and formation of anatase TiO_2 [28]. The cation species formed in the hydrolysis of TiF_6^{2-} is thought to be ion-exchanged with cation (H^+ or NH_4^+) in Nafion membrane and dehydrolyzed to TiO_2 in membrane inner region as shown in Fig. 5. The concentration of $\text{Ti(OH)}_2\text{F}^+$ ion is much poor in the $(\text{NH}_4)_2\text{TiF}_6$ aqueous solution (not formation of TiO_2 in the system) due to the low equilibrium constant $K \sim 10^{-13}$ [27], which is confirmed by XPS study shown later. Such cation might form in the solution phase in the initial condition.

The SAXS profiles of the modified and unmodified membranes at various TiO_2 deposition times are shown in Fig. 6. The broadened peak around $q = 1.7\text{--}1.8 \text{ nm}^{-1}$ is assigned to ionic clusters in the membrane structure. Increasing scattering intensity at small q value ($q = 0.1\text{--}1 \text{ nm}^{-1}$) is due to the scattering of deposited TiO_2 .

The peak intensity of ionomer decreases with increasing reaction period. We speculated that the decreasing peak intensity for reaction periods is caused by the presence of TiO_2 within the ionic

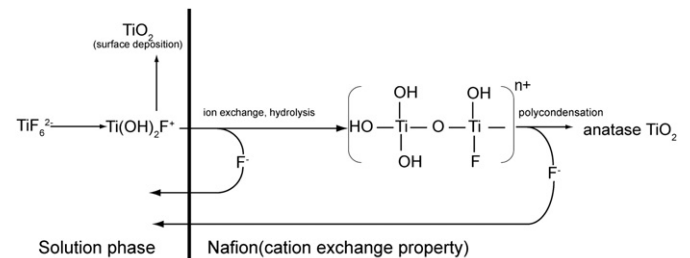


Fig. 5. Schematic illustration of hydrolysis reaction of TiF_6^{2-} for Nafion membrane.

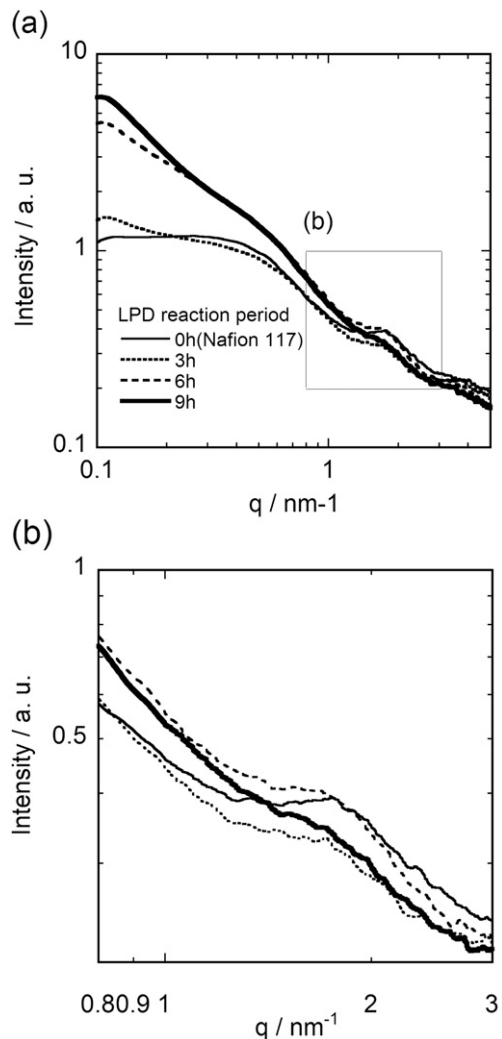


Fig. 6. (a) SAXS profiles of the modified membrane at various reaction periods. (b) Enlarge image for the part of the square indicated in (a).

clusters, thereby resulting in a poorly ordered water retention network in Nafion 117. Similar results were obtained in a previous study by Mauritz [13]. Increasing the amount of TiO₂ resulting in the increasing scattering intensity at below $q = 1 \text{ nm}^{-1}$ and decreasing the intensity at $q = 1.7\text{--}1.8 \text{ nm}^{-1}$ indicate the deposition occurred in the ionic clusters of Nafion membrane.

The ionic clusters serve as a pathway for the migration of the deposited TiO₂ in the Nafion membrane. During the LPD process, the Nafion membrane remains fully hydrated since the reaction occurs in an aqueous medium. Such an environment is beneficial to the migration of the deposited species from the surface to the inner regions of the membrane. SAXS results revealed TiO₂ nanoparticles which confirmed in the TEM images present in the ionic clusters of Nafion membrane.

We carried out XPS studies in order to investigate the site distribution of TiO₂ in the Nafion membrane.

The XPS spectra of TiO₂-Nafion as followed the process of experimental section recorded after each etching by Ar⁺ gun are shown in Fig. 7a. Because the Ar⁺ that was used for etching affects the membrane's chemical state (particularly the Ti species), Ti⁴⁺ was reduced to an oxidized state by the effects of the Ar⁺ bombardment [29]. This effect was reflected as the photoelectron signal present between 450 eV and 460 eV. In the F1s XPS spectra shown in Fig. 7b, two species at least are observed between 680 eV and 690 eV in binding energy. The peak in the higher binding energy at 689 eV is perfluoro group in Nafion and in the lower binding energy at 684 eV is F⁻ ion in the deposition [30]. The origin of F⁻ ion may be contribution from the surface of TiO₂ nanoparticles, which indicates that the hydrolysis reaction occurs in the Nafion membrane.

We plotted the integral intensity curves that represent the amount of Ti without considering its oxidation state. These integral intensities are summarized in Fig. 8. The shorter the reaction period (3 and 6 h in the figure), the more are the changes in the distribution in the distance from the membrane surface. These tendencies correspond with the TEM depth profile. In the early reaction period, the neutral or cation species such as TiF₄ and Ti(OH)₂F⁺ hydrolyzed to TiO₂ immediately in the ionic clusters. Meanwhile in the later period, since the bound water by TiO₂ might have less activity concerning the hydrolysis reaction of fluoro

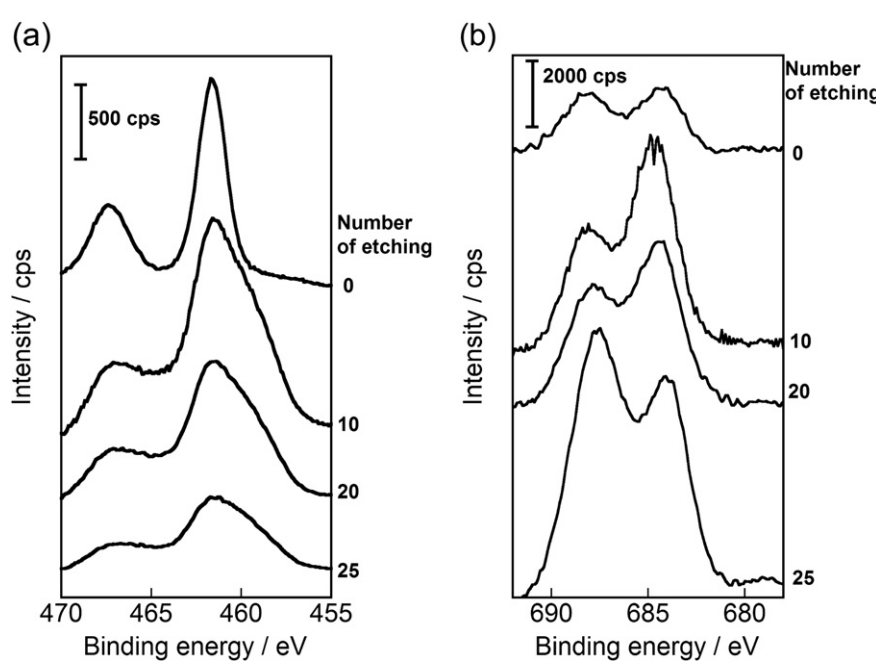


Fig. 7. XPS spectra of (a) Ti and (b) F species in the membrane after 9 h of reaction after Ar⁺ etching.

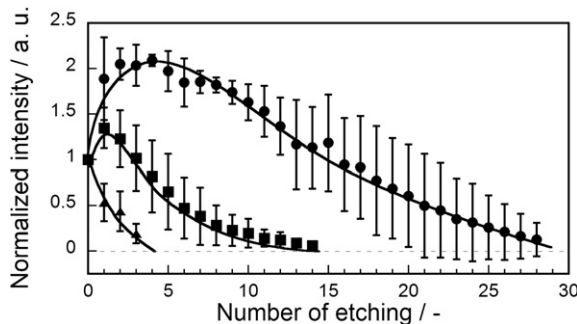


Fig. 8. XPS depth profile of Ti species in the membrane after various reaction periods; triangle (\blacktriangle) 3 h square (\blacksquare) 6 h and circle (\bullet) 9 h of reaction period.

complexes, the diffusion was promoted due to the presence with longer period of diffusion species such as TiF_4 and $\text{Ti}(\text{OH})_2\text{F}^+$.

We also attempted Nafion membrane modification by LPD without the addition of H_3BO_3 as an F^- scavenger as explained in **Introduction** section. The XPS spectra revealed no presence of Ti species in the membrane. This absence of Ti^{4+} cation is evidence of the non-incorporation of TiO_2 nanoparticles in the membrane. On the one hand, it is considered that in the absence of H_3BO_3 , the hydrolysis reaction of the metal fluoro-complex does not occur. Consequently, there is no deposition of metal oxide. On the other hand, the anionic repulsion of the sulfonic acid group from the Nafion membrane and the metal fluoro-complex is thought to be so strong that TiF_6^{2-} complex remains imperturbable. These two factors prevent the deposition reaction from occurring in the Nafion membrane, and they underline the crucial role of H_3BO_3 in the LPD reaction mechanism [18].

In order to examine the influence of diffusion from the bulk phase of TiO_2 colloidal particles, we prepared TiO_2 colloidal solution by aging of mix solution of $(\text{NH}_4)_2\text{TiF}_6$ and H_3BO_3 for 9 h and immersed pure Nafion into this solution for 30 min. Subsequently, we could not observe the $\text{Ti}2\text{p}$ photoelectron in the binding energy for the membrane.

3.3. Water retention properties of TiO_2 -dispersed Nafion membrane

The TGA profiles of the modified and unmodified membranes at various reaction periods are shown in Fig. 9a. Three prominent temperature regions can be observed—region (i) ca. 80 °C at which the conventional PEFCs were operated, region (ii) 100–250 °C at which the dehydration of Nafion occurred, and region (iii) over 250 °C at which the membrane degraded. In this section, we discuss the dependence of the weight loss in Nafion 117 due to water evaporation from the membrane in the LPD reaction, i.e., TiO_2 deposition time onto the Nafion membrane.

It is obvious that the weight loss in Nafion 117 occurs faster than that for the composite-membranes in all the abovementioned temperature regions. The 3 h LPD-modified composite shows the second fastest weight loss. The 6 h LPD-modified membrane exhibits a slower water loss than the LPD-modified 9 h membrane in region (i); however, the curve rapidly falls beyond 150 °C. The corresponding water evaporation behavior of the membranes at 80, 100, and 200 °C as a function of reaction period is plotted in Fig. 9b.

Firstly, it is clear that the membrane's water holding capacity shows a similar behavior for all three temperatures (80, 100, and 200 °C). The water retention capacity monotonously increases up to 6 h of reaction period; thereafter, no significant change is observed. We speculate that after 6 h, the deposition of TiO_2 in the Nafion ionic cluster has almost completed. Therefore, any further increase in reaction period only favors the assembling of TiO_2 nanoparticles

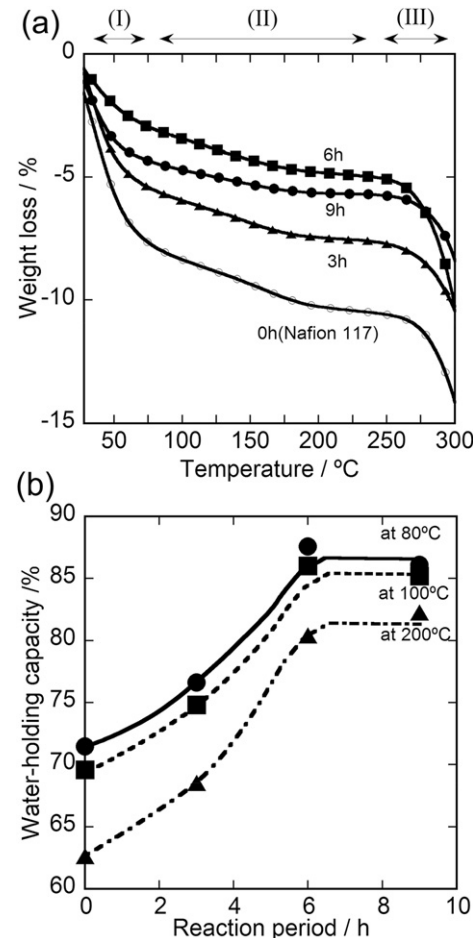


Fig. 9. Variation in water evaporation of Nafion- TiO_2 composite as a function of: (a) temperature; solid line (—) Nafion 117, triangle (\blacktriangle) 3 h square (\blacksquare) 6 h and circle (\bullet) 9 h of reaction period. (b) As a function of reaction period; circle (\bullet) 80 °C, square (\blacksquare) 100 °C and triangle (\blacktriangle) 200 °C.

aggregations at the surface of the membrane. The water retention amount was improved from 63% to 83% at 200 °C due to TiO_2 deposition, whose weight ratio is only 0.11 wt% in the LPD deposition reaction that was carried out for 6 h. This loaded amount is much less than that used in conventional synthesis [7–16]; the quantities of inorganic fillers in general range from 2.5 wt% to 23 wt %. We recorded also the weight loss by TG apparatus whose

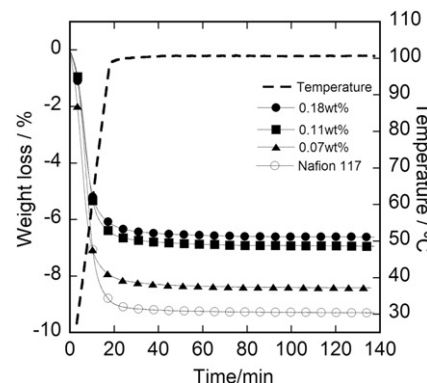


Fig. 10. Time dependence of weight loss of TiO_2 -dispersed membrane at 100 °C. Dashed line represents the temperature, the symbols of (\circ) Nafion 117, (\blacktriangle) 3 h (0.07 wt%), (\blacksquare) 6 h (0.11 wt%), (\bullet) 9 h (0.18 wt%) TiO_2 , respectively.

temperature condition in atmosphere was kept at 100 °C after heating in 5 K min⁻¹ from room temperature. The weight loss of fully hydrated membrane was plotted in Fig. 10. The weight losses are similar to the value expected with the water holding capacity

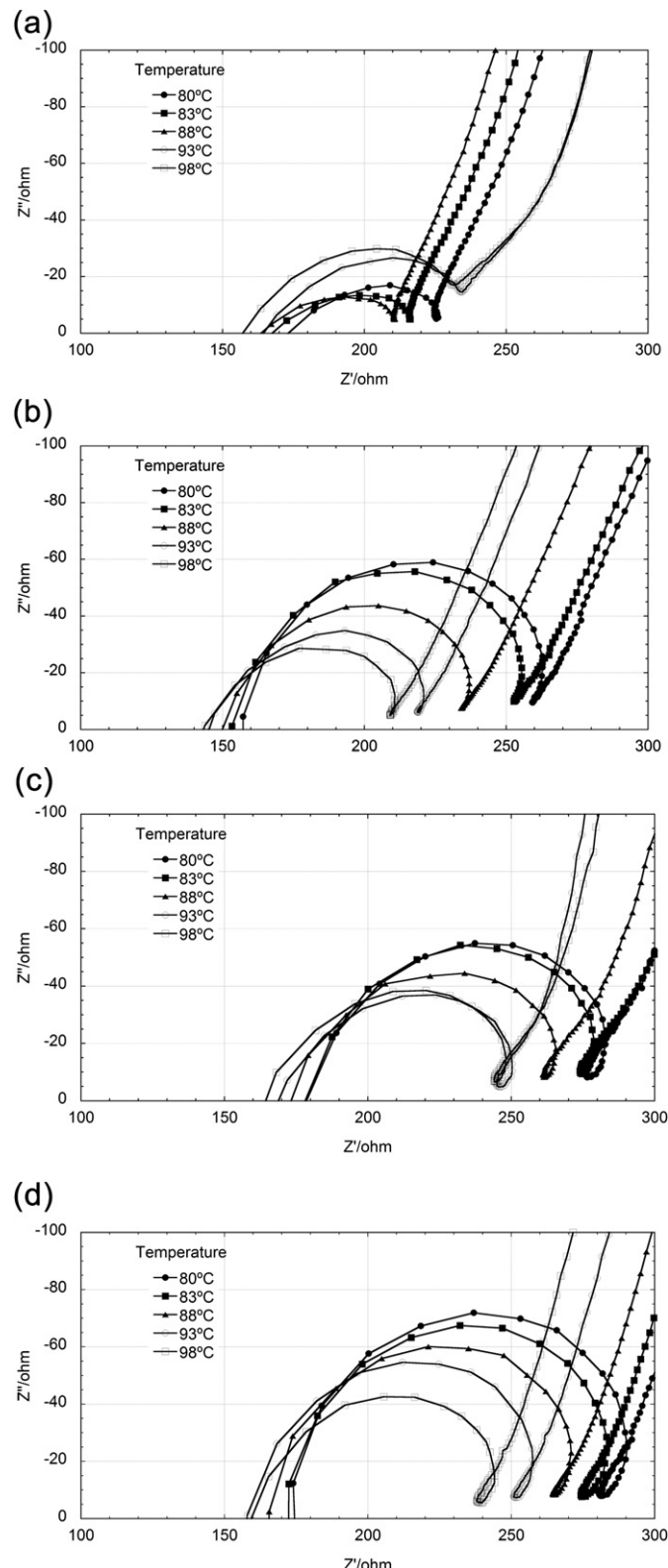


Fig. 11. Nyquist plots of membrane samples at various temperatures; (a) Nafion 117, (b) after LPD reaction for 3 h, (c) 6 h, and (d) 9 h. The numbers in inset correspond to frequency.

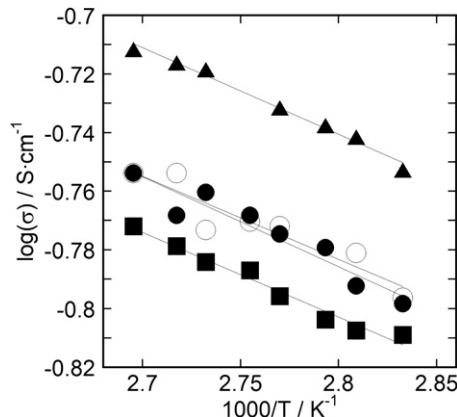


Fig. 12. Arrhenius plot of conductivity σ calculated from R component with temperature for TiO_2 /Nafion composite membrane. TiO_2 content: (○) 0 wt% (original), (▲) 0.07 wt%, (■) 0.11 wt%, (●) 0.18 wt%.

for all membrane samples and hardly changed after aging at 100 °C even after 120 min.

This indicates the TiO_2 nanoparticles in the membrane play retention of water molecules well at high temperature.

3.4. Conductivity measurement of Nafion with TiO_2 nanoparticles

Typical impedance plots obtained using the sample of original Nafion and TiO_2 -dispersed Nafion membranes at the various temperatures are shown in Fig. 11. The logarithm of σ had linear dependence on the reciprocal absolute temperature over measured range (Arrhenius plot) was shown in Fig. 12. The similar gradients indicate the bulk conductance of all membrane samples have similar activation energy (around 5.5 kJ mol⁻¹) to that of Nafion 117 and LPD modified membrane. Otherwise, the 0.07 wt% TiO_2 loaded Nafion membrane has superior conductivity compared with other membrane including Nafion 117. Such enhancement of the conductivity is due to nanoparticles confined in the Nafion's cluster at the vicinity of surface, which enroll retention of water because the major TiO_2 exist as nanoparticles. On the other side, more than 0.11 wt% TiO_2 loaded Nafion membrane have same or smaller conductivity to Nafion 117. This is because the extra amount of TiO_2 impedes the conduction of proton. We can conclude LPD process is suitable for improving water management due to small amount of TiO_2 nanoparticles at the vicinity of the membrane surface.

4. Conclusion

In our study, TiO_2 -dispersed Nafion membrane was prepared by the liquid phase deposition method at room temperature. The obtained membrane showed TiO_2 dispersion in the weight range of 0.07–0.18 wt% at and below the surface of the membrane. The dispersion conditions of TiO_2 were observed by TEM and XPS. A relatively small amount of TiO_2 nanoparticles were successfully dispersed in the Nafion 117 membrane with a distribution vicinity of the surface. The deposition mechanism is suggested as the ion exchange phenomena. The spatial distribution is contributed from the bound water by the TiO_2 in the Nafion membrane. The TiO_2 nanoparticles in the membrane grew and aggregated in clusters; the aggregation at the surface resulted in the formation of a film with increase in reaction period. The amount of water retention was improved from 63% to 83% at 200 °C due to TiO_2 deposition; the weight ratio of the deposited TiO_2 was merely 0.18 wt% when compared with that for conventional methods.

In further study, we are going to measure the performance in practical fuel cell operation. We believe that the use of such a hybrid material as a membrane can improve the operation of PEFCs at higher temperature due to the material's high water retention properties.

Acknowledgments

The authors would like to thank Professor Hideto Matsuyama and Dr. Cui Liang for their discussions regarding the measurements of the proton conductivity using electrical cells and the water retention of the fabricated TiO₂-dispersed Nafion membrane.

References

- [1] N.Y. Steiner, P.Ph. Moçotéguy, D. Candusso, D. Hissel, *J. Power Sources* 194 (2009) 130.
- [2] S.J. Peighambarioust, S. Rowshanzamir, M. Amjadi, *Int. J. Hydrogen Energy* 35 (2010) 9349.
- [3] V. Mehta, J.S. Cooper, *J. Power Sources* 114 (2003) 32.
- [4] S. Gottesfeld, T.A. Zawodzinski, *Adv. Electrochem. Sci. Eng.* 5 (1997) 195.
- [5] H. Xua, Y. Songa, H.R. Kunz, J.M. Fenton, *J. Power Sources* 159 (2006) 979.
- [6] Y. Shao, G. Yin, Z. Wang, Y. Gao, *J. Power Sources* 167 (2007) 235.
- [7] V.D. Noto, R. Gliubizzi, E. Negro, M. Vittadello, G. Pace, *Electrochim. Acta* 53 (2007) 1618.
- [8] N.H. Jalani, K. Dunn, R. Datta, *Electrochim. Acta* 51 (2005) 553.
- [9] Z.G. Shao, H. Xu, M. Li, I.M. Hsing, *Solid State Ionics* 177 (2006) 779.
- [10] E.I. Santiago, R.A. Isidoro, M.A. Dresch, B.R. Matos, M. Linardi, F.C. Fonseca, *Electrochim. Acta* 54 (2009) 4111.
- [11] Y. Patil, S. Sanbandam, V. Ramani, K. Mauritz, *J. Electrochem. Soc.* 156 (2009) B1092.
- [12] A.K. Sahu, G. Selvarani, S. Pitchumani, P. Sridhar, A.K. Shukla, *J. Electrochem. Soc.* 154 (2007) B123.
- [13] K.A. Mauritz, I.D. Stefanithis, S.V. Davis, R.W. Scheetz, R.K. Pope, G.L. Wilkes, H.H. Huang, *J. Appl. Poly. Sci.* 55 (1995) 181.
- [14] Y.S. Park, Y. Yamazaki, *J. Membr. Sci.* 261 (2005) 58.
- [15] M. Watanabe, H. Uchida, Y. Seki, M. Emori, *J. Electrochem. Soc.* 143 (1996) 3847.
- [16] K.T. Park, U.H. Jung, D.W. Choi, K. Chun, H.M. Lee, S.H. Kim, *J. Power Sources* 177 (2008) 247.
- [17] H. Nagayama, H. Honda, H. Kawahara, *J. Electrochem. Soc.* 135 (1988) 2013.
- [18] S. Deki, Y. Aoi, O. Hiroi, A. Kajinami, *Chem. Lett.* (1996) 433.
- [19] S. Deki, S. Iizuka, A. Horie, M. Mizuhata, A. Kajinami, *Chem. Mater.* 16 (2004) 1747.
- [20] M. Mizuhata, T. Miyake, Y. Nomoto, S. Deki, *Microelectron. Eng.* 85 (2008) 355.
- [21] S. Iizuka, S. Ooka, A. Nakata, M. Mizuhata, S. Deki, *Electrochim. Acta* 51 (2004) 802.
- [22] S. Deki, A. Nakata, M. Mizuhata, *Electrochemistry* 72 (2004) 452.
- [23] S. Deki, A. Nakata, M. Mizuhata, *ECS Trans.* 3 (2006) 29.
- [24] T. Hasegawa, S. Matsumoto, M. Mizuhata, *Chem. Lett.* 41 (2012) 1262.
- [25] M. Mizuhata, Y. Kodama, S. Deki, *J. Ceram. Soc. Jpn.* 117 (2009) 326.
- [26] T.A. Zawodzinski, M. Neeman, L.O. Sillerud, S. Gottesfeld, *J. Phys. Chem.* 95 (1991) 6040.
- [27] L. Ciavatta, A. Pirozzi, *Polyhedron* 2 (1983) 769.
- [28] T. Sugimoto, X. Zhou, A. Muramatsu, *J. Colloid Interface Sci.* 252 (2002) 339.
- [29] S. Hashimoto, A. Tanaka, *Surf. Interface Anal.* 34 (2004) 262.
- [30] J.G. Yu, H.G. Yu, B. Cheng, X.J. Zhao, J.C. Yu, W.K. Ho, *J. Phys. Chem. B* 107 (2003) 13871.